Polarization-dependent continuous change in the propagation direction of Dirac-cone modes in photonic-crystal slabs

Kazuaki Sakoda

Photonic Materials Unit, National Institute for Materials Science, 1-1 Namiki, Tsukuba, Ibaraki 305-0044, Japan
and Graduate School of Pure and Applied Sciences, University of Tsukuba, 1-1-1 Tennodai, Tsukuba, Ibaraki 305-8571, Japan

(Received 1 July 2014; published 28 July 2014)

We show that the propagation direction of the Dirac-cone modes of photonic-crystal slabs can be continuously controlled by the polarization of the incident wave. This property is realized by their isotropic dispersion relation and anisotropic mixture of two dipolar wave functions. To clarify these features, we formulate a Green-function method to describe the excitation process of the Dirac-cone modes and analyze the coupling strength with the incident wave by group theory. This angular dependence of the intensity distribution of the excited wave can be used for experimentally detecting the Dirac cones and distinguishing their mode symmetry.

DOI: 10.1103/PhysRevA.90.013835 PACS number(s): 42.70.Qs, 78.67.Pt, 81.05.Xj

I. INTRODUCTION

Since the discovery of topological photonic states and their relevant novel optical phenomena, the search and materialization of photonic Dirac cones has become one of the most active research fields of optics [1–9]. Haldane *et al.* [1,2] pointed out the presence of the Dirac cone on the K point of the Brillouin zone of a triangular-lattice photonic crystal and discussed the unidirectional propagation of surface optical waves in the system without the time-reversal symmetry. Ochiai *et al.* extended the discussion to the honeycomb lattice [3]. The Dirac-cone dispersion also materializes optical simulation of *Zitterbewegung*, or trembling motion, in particle physics by propagating an optical pulse of the Dirac point frequency [4,5] and the pseudodiffusive transmission, which was found by Sepkhanov *et al.* [6] and numerically demonstrated by Diem *et al.* [7]. Wang *et al.* observed the unidirectional propagation of surface waves in the microwave frequency range [8] and Hafezi *et al.* materialized an analogous unidirectional propagation by a two-dimensional microcavity array based on the silicon photonics [9].

In addition to the deterministic formation of the Dirac cone on the boundary of the Brillouin zone, it can also be materialized on the Γ point (Brillouin-zone center) by accidental degeneracy, as was shown by Huang *et al.* [10]. Then, Mei *et al.* discussed the formation of Dirac cones, Berry phase, and mapping into the Dirac Hamiltonian for phononic and photonic crystals by the $\mathbf{k}\cdot\mathbf{p}$ perturbation theory [11]. Because the Dirac point in the Brillouin-zone center is equivalent to a zero effective refractive index [10], it has much potential for various applications such as scatter-free waveguides [12] and lenses of arbitrary shapes [13].

On the other hand, we showed by tight-binding approximation and group theory that Dirac cones can also be created by accidental degeneracy in the Brillouin-zone center of metamaterials, which are characterized by well-defined electromagnetic resonant states localized in their unit structures [14,15]. We proved the presence of isotropic Dirac cones with auxiliary quadratic dispersion surfaces in square-, triangular-, and simple-cubic-lattice metamaterials [Fig. 1(a)] and the presence of the double Dirac cone, or a pair of identical Dirac cones, in the triangular-lattice metamaterials [Fig. 1(b)]. We also applied the $\mathbf{k}\cdot\mathbf{p}$ perturbation theory and group theory to this problem and showed that the structure of the first-order perturbation matrix is determined almost uniquely by the mode symmetry, and completely clarified the conditions for obtaining the Dirac cones [16].

In this paper, we analyze photonic crystal slabs, which are the best candidate for materializing the photonic Dirac cones in the optical frequencies. In particular, we analyze the coupling strength between the incident wave and the Dirac-cone modes by group theory and show that the propagation direction of the slab mode can be controlled by the polarization of the incident wave. This paper is organized as follows. In Sec. II, we analyze the excitation process of the Dirac-cone modes by an incident monochromatic plane wave and calculate Poynting's vector of the induced wave running parallel to the slab surface. In Sec. III, we apply this method to the square-lattice photonic-crystal slab and show the peculiar polarization-angle dependence of the propagation direction. The Dirac cone and double Dirac cone in the triangular lattice are analyzed in Sec. IV. A summary of the present study is given in Sec. V. A retarded Green function for the magnetic field is derived in Appendix A. In Appendix B, plane-wave radiation by oscillating magnetic polarization in free space is formulated by the Green-function method.

II. COUPLING WITH AN INCIDENT PLANE WAVE

By using the retarded Green function for the magnetic field, which is formulated in Appendix A, we examine the excitation process of Dirac-cone modes by an incident plane wave, which we denote by $\mathbf{H}_{\rm in}$:

$$\mathbf{H}_{\rm in}(\mathbf{r},t) = \mathbf{H}_0 e^{i(\mathbf{k}_0\cdot\mathbf{r}-\omega t)}, \tag{1}$$

where $\mathbf{k}_0$ and ω are the wave vector and angular frequency of the incident wave. So, $\omega = c|\mathbf{k}_0|$, where c is the velocity of light in free space. To analyze this process by means of Eq. (A15), we introduce a uniform planar distribution of virtual oscillating magnetic dipoles that generate the plane wave $\mathbf{H}_{\rm in}$, which are located sufficiently far from the photonic-crystal slab and are denoted by $\mathbf{P}_m$:

$$\mathbf{P}_m = \mathbf{d}_m \delta(z - z_0) e^{i(\kappa_x x + \kappa_y y) + (-i\omega + \delta)t}, \tag{2}$$

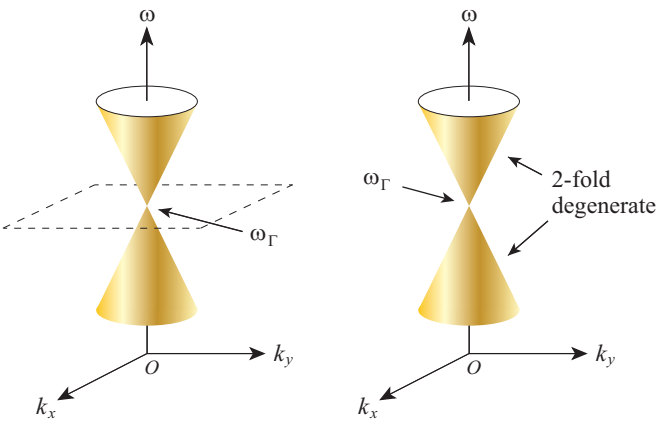

FIG. 1. (Color online) (a) Dirac cone (gold) with an auxiliary dispersion surface (dotted lines), and (b) double Dirac cone on the Γ point ($\mathbf{k} = 0$) of the two-dimensional Brillouin zone materialized by accidental degeneracy of two modes with particular combinations of mode symmetries. At the degenerate frequency denoted by ω_Γ, which is called the Dirac point, the effective refractive index is equal to zero.

where Cartesian coordinates are used as shown in Fig. 2. z_0, which we assume to be positive without loss of generality, is a constant much larger than the wavelength of the incident wave, $2\pi c/\omega$. For simplicity, we assume that $\mathbf{d}_m$ is perpendicular to the z axis and denote its tilt angle against the x axis by θ (Fig. 3). In Eq. (2), positive infinitesimal δ was introduced to assure the adiabatic switching of the oscillation. κ_x and κ_y are the x and y components of the wave vector of the incident wave $\mathbf{k}_0$:

$$\mathbf{k}_0 = \left(\kappa_x,\, \kappa_y,\, -\sqrt{\omega^2/c^2 - \kappa_x^2 - \kappa_y^2}\,\right). \tag{3}$$

The inhomogeneous equation with $\mathbf{P}_m$ as a source term is given by

$$-\left(\frac{1}{c^2}\frac{\partial^2}{\partial t^2} + \mathcal{L}_H\right)\mathbf{H}(\mathbf{r},t) = \varepsilon_0 \frac{\partial^2 \mathbf{P}_m}{\partial t^2}, \tag{4}$$

where differential operator $\mathcal{L}_H$ is defined by Eq. (A4). From Eq. (A15), we obtain

$$\begin{aligned}\mathbf{H}(\mathbf{r},t) &= \int_V d\mathbf{r}' \int_{-\infty}^{\infty} dt'\, \mathrm{G}(\mathbf{r},\mathbf{r}',t-t')\varepsilon_0 \frac{\partial^2}{\partial t'^2}\mathbf{P}_m(\mathbf{r}',t') \\ &= -\frac{\mathbf{P}_m(\mathbf{r},t)}{\mu_0} + \sum_{\mathbf{k}n} \frac{\omega_{\mathbf{k}n}\mathbf{H}^{(T)}_{\mathbf{k}n}(\mathbf{r})}{\mu_0 V} \int_V d\mathbf{r}' \int_{-\infty}^{t} dt' \\ &\quad \times \mathbf{H}^{(T)*}_{\mathbf{k}n}(\mathbf{r}') \cdot \mathbf{P}_m(\mathbf{r}',t') \sin \omega_{\mathbf{k}n}(t-t'),\end{aligned} \tag{5}$$

where μ_0 is the permeability of free space, V is the volume on which the periodic boundary condition is imposed, and $\omega_{\mathbf{k}n}$ and $\mathbf{H}^{(T)}_{\mathbf{k}n}(\mathbf{r})$ are the eigenangular frequency and the magnetic field eigenfunction of the transverse mode with wave vector $\mathbf{k}$ and band index n. So, the propagating part of the induced wave is given only by the transverse waves and the longitudinal waves were used to reconstruct the original oscillating polarization.

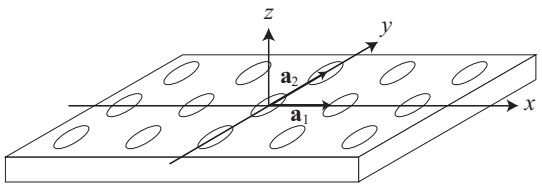

FIG. 2. Illustration of the square-lattice photonic-crystal slab of the C_{4v} symmetry, which is composed of a regular array of circular air cylinders fabricated in a uniform dielectric slab. Because the two-dimensional C_{4v} symmetry is sufficient for the Dirac cone, we do not assume a mirror symmetry about the horizontal middle plane.

For free space,

$$\mathbf{H}^{(T)}_{\mathbf{k}n}(\mathbf{r}) = \mathbf{h}_{\mathbf{k}} e^{i\mathbf{k}\cdot\mathbf{r}} \quad (\mathbf{h}_{\mathbf{k}} \cdot \mathbf{k} = 0), \tag{6}$$

$$\omega_{\mathbf{k}n} = c|\mathbf{k}|, \tag{7}$$

where $\mathbf{h}_{\mathbf{k}}$ is a unit vector perpendicular to $\mathbf{k}$. In this equation, $\mathbf{k}$ is a general wave vector in the three-dimensional reciprocal space that is not restricted to the two-dimensional first Brillouin zone of the photonic-crystal slab, so we omitted subscript n. Then, from Eq. (5), we can derive the formula for the plane wave emitted by the oscillating magnetic polarization, the details of which are given in Appendix B. The emitted wave is given by Eq. (1), where $\mathbf{H}_0$ is a vector perpendicular to $\mathbf{k}$ and parallel to the plane spanned by $\mathbf{d}_m$ and $\mathbf{k}$. For emission in the normal direction in particular, that is, for $\kappa_x = \kappa_y = 0$, its amplitude is

$$|\mathbf{H}_0| = \frac{\omega|\mathbf{d}_m|}{2\mu_0 c}. \tag{8}$$

Now, we go back to the problem of the excitation process of the Dirac-cone modes. First, from the Bloch theorem, each eigenfunction of the magnetic field is a product of an exponential function and a periodic vectorial function:

$$\mathbf{H}^{(T)}_{\mathbf{k}n}(\mathbf{r}) = e^{i\mathbf{k}\cdot\mathbf{r}}\mathbf{u}_{\mathbf{k}n}(\mathbf{r}), \tag{9}$$

$$\mathbf{u}_{\mathbf{k}n}(\mathbf{r} + \mathbf{a}_i) = \mathbf{u}_{\mathbf{k}n}(\mathbf{r}) \quad (i = 1, 2), \tag{10}$$

where $\mathbf{a}_i$ ($i = 1, 2$) is an elementary lattice vector parallel to the surface of the photonic-crystal slab. Second, the summation over n in Eq. (5) includes two types of eigenmodes. One is the waveguide modes localized on the photonic-crystal slab, and

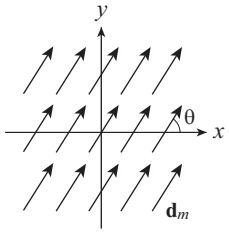

FIG. 3. Distribution of the oscillating magnetic polarization with amplitude $\mathbf{d}_m$ and tilt angle θ. It has a phase factor $e^{i(\kappa_x x + \kappa_y y)}$ to produce a plane wave propagating in the direction designated by $\mathbf{k}_0 = (\kappa_x, \kappa_y, -\sqrt{\omega^2/c^2 - \kappa_x^2 - \kappa_y^2})$.

the other is reflected, transmitted, and diffracted waves that propagate like plane waves when they are sufficiently away from the slab and do not have a large amplitude in the vicinity of the slab. The former have discrete eigenfrequencies for each (κ_x,κ_y) and compose the Dirac cone. On the other hand, the latter have quasicontinuous eigenfrequencies that may be designated by the z component of the wave vector. Because we are interested only in the former, we ignore the contribution from the latter.

Then we replace the summation over n by a summation over waveguide modes in the relevant frequency range, which we distinguish by j. When we substitute Eq. (9) and omit the source term (the first term on the right-hand side), Eq. (5) gives the propagating part of the magnetic field as follows:

$$\mathbf{H}(\mathbf{r},t) \approx \sum_{j=1}^{n_s} \frac{\omega_{\kappa j}\mathbf{H}_{\kappa j}^{(T)}(\mathbf{r})\langle \mathbf{u}_{\kappa j}^*(z_0)\cdot\mathbf{d}_m\rangle_0 e^{-i\omega t}}{2\mu_0} \times\left(\frac{1}{\omega+\omega_{\kappa j}+i\delta}-\frac{1}{\omega-\omega_{\kappa j}+i\delta}\right), \quad (11)$$

where

$$\kappa = (\kappa_x,\kappa_y,0), \quad (12)$$

n_s is the number of the slab modes that contribute to the Dirac cone, and $\langle \mathbf{u}_{\kappa j}^*(z_0)\cdot\mathbf{d}_m\rangle_0$ is defined by

$$\langle \mathbf{u}_{\kappa j}^*(z_0)\cdot\mathbf{d}_m\rangle_0 = \frac{1}{V}\int_V d\mathbf{r}\,\mathbf{u}_{\kappa j}^*(\mathbf{r})\cdot\mathbf{d}_m\delta(z-z_0). \quad (13)$$

To excite the waveguide mode by an incident plane wave, the wave vector parallel to the slab surface and the frequency have to be tuned exactly. But this exact tuning is practically impossible, so instead we have to assume a finite width of the eigenfrequency, which is brought about by the finite lifetime of the eigenmode due to dielectric loss, diffraction, etc. Thus we replace the positive infinitesimal δ by a nonzero relaxation rate γ in Eq. (5) and ignore the counter resonant term (the first term) in the parentheses.

To calculate the electromagnetic energy flux, we evaluate the divergence of the time average of Poynting's vector $\overline{\mathbf{S}}$:

$$\begin{aligned}\nabla\cdot\overline{\mathbf{S}(\mathbf{r},t)} &= \frac{1}{4}\nabla\cdot[\mathbf{E}(\mathbf{r},t)\times\mathbf{H}^*(\mathbf{r},t)+\mathbf{E}^*(\mathbf{r},t)\times\mathbf{H}(\mathbf{r},t)]\\ &= \frac{i\omega\delta(z-z_0)}{4}\sum_j^{n_s}\left[\frac{\alpha_{\kappa j}\mathbf{u}_{\kappa j}(\mathbf{r})\cdot\mathbf{d}_m^*}{\omega-\omega_{\kappa j}+i\gamma_{\kappa j}}\right.\\ &\quad\left.-\frac{\alpha_{\kappa j}^*\mathbf{u}_{\kappa j}^*(\mathbf{r})\cdot\mathbf{d}_m}{\omega-\omega_{\kappa j}-i\gamma_{\kappa j}}\right], \end{aligned} \quad (14)$$

where $\alpha_{\kappa j}$ is defined as

$$\alpha_{\kappa j} = \frac{\omega_{\kappa j}}{2\mu_0}\langle \mathbf{u}_{\kappa j}^*(z_0)\cdot\mathbf{d}_m\rangle_0. \quad (15)$$

So, the electromagnetic energy radiated in a unit time and a unit volume, which we denote by $\dot{U}$, is

$$\dot{U} = \frac{1}{V}\int_V d\mathbf{r}\nabla\cdot\overline{S(\mathbf{r},t)} \approx \mu_0\sum_{j=1}^{n_s}\frac{|\alpha_{\kappa j}|^2\gamma_{\kappa j}}{(\omega-\omega_{\kappa j})^2+\gamma_{\kappa j}^2}. \quad (16)$$

Now, we assume that the quality factor of the Dirac-cone modes is sufficiently large, so its energy flux is nearly parallel to the slab surface. Then, its energy velocity, which is equal to the group velocity $\mathbf{v}_{\kappa j}$ in the case of lossless media [18], is given by the slope of the Dirac cone. As a result, the energy flux in the slab plane, $\mathbf{S}_\parallel$, is

$$\mathbf{S}_\parallel = \mu_0 L_z\sum_{j=1}^{n_s}\frac{|\alpha_{\kappa j}|^2\gamma_{\kappa j}\mathbf{v}_{\kappa j}}{\{(\omega-\omega_{\kappa j})^2+\gamma_{\kappa j}^2\}|\mathbf{v}_{\kappa j}|}, \quad (17)$$

where L_z is the size of volume V in the z direction. In the following sections, we calculate $\mathbf{S}_\parallel$ for the square-lattice and triangular-lattice photonic-crystal slabs.

III. SQUARE LATTICE OF C_{4v} SYMMETRY

We start with a photonic-crystal slab of the C_{4v} symmetry, i.e., the symmetry of the regular square (see Fig. 2). The condition to materialize Dirac cones for this symmetry was analyzed by the tight-binding approximation [14] and by the vector $\mathbf{k}\cdot\mathbf{p}$ perturbation theory [16]. We can create a Dirac cone with an auxiliary quadratic dispersion surface by the combination of an E mode and an A_1, A_2, B_1, or B_2 mode. First, we examine the combination of an E (dipolar) mode and an A_1 (monopolar) mode as an example.

From the analysis by the vector $\mathbf{k}\cdot\mathbf{p}$ perturbation theory [16], the wave function and the eigenfrequency of the eigenmodes in the degenerate condition are given by solving the following eigenequation:

$$\begin{pmatrix}0, & 0, & bk_x\\ 0, & 0, & bk_y\\ b^*k_x, & b^*k_y, & 0\end{pmatrix}\begin{pmatrix}A\\B\\C\end{pmatrix} = \Delta\lambda\begin{pmatrix}A\\B\\C\end{pmatrix}, \quad (18)$$

where $\lambda=\omega^2/c^2$ and $\Delta\lambda$ denote the difference between the modes for $\mathbf{k}\neq 0$ and for $\mathbf{k}=0$. The eigenwave function is then given by

$$\mathbf{u}_\mathbf{k} = A\mathbf{u}_E^{(1)} + B\mathbf{u}_E^{(2)} + C\mathbf{u}_{A_1}, \quad (19)$$

where $\mathbf{u}_E^{(1)}$ and $\mathbf{u}_E^{(2)}$ are two wave functions of the doubly degenerate E mode on the Γ point ($\mathbf{k}=0$), the former of which transforms like the x coordinate and the latter transforms like the y coordinate when symmetry operations of the C_{4v} point group are conducted [19]. $\mathbf{u}_{A_1}$ is the wave function of the A_1 mode on the Γ point, which is invariant by any of the symmetry operations of the C_{4v} point group [19]. Parameter b is given by

$$b = i\mathbf{e}_x\cdot\left[-\langle\mathbf{u}_E^{(1)}|\Delta\mathcal{L}|\mathbf{u}_{A_1}\rangle_0+\langle\mathbf{u}_{A_1}|\Delta\mathcal{L}|\mathbf{u}_E^{(1)}\rangle_0^*\right], \quad (20)$$

where

$$\Delta\mathcal{L} = \times\left[\frac{1}{\varepsilon(\mathbf{r})}\nabla\times\right], \quad (21)$$

and $\mathbf{e}_x$ is a unit vector in the positive x direction.

The eigenvalues of Eq. (18) are

$$\Delta\lambda = 0, \quad \pm|b|k, \quad (22)$$

where $k=\sqrt{k_x^2+k_y^2}$. The solutions for $\lambda=\pm|b|k$ form the Dirac cone and that for $\lambda=0$ gives the quadratic dispersion surface. The three solutions are given as follows:

(i) $\Delta\lambda = 0$

$$\begin{pmatrix} A^{(0)} \\ B^{(0)} \\ C^{(0)} \end{pmatrix} = \begin{pmatrix} \sin\phi \\ -\cos\phi \\ 0 \end{pmatrix}, \tag{23}$$

(ii) $\Delta\lambda = |b|k$

$$\begin{pmatrix} A^{(+)} \\ B^{(+)} \\ C^{(+)} \end{pmatrix} = \frac{1}{\sqrt{2}} \begin{pmatrix} e^{i\beta}\cos\phi \\ e^{i\beta}\sin\phi \\ 1 \end{pmatrix}, \tag{24}$$

(iii) $\Delta\lambda = -|b|k$

$$\begin{pmatrix} A^{(-)} \\ B^{(-)} \\ C^{(-)} \end{pmatrix} = \frac{1}{\sqrt{2}} \begin{pmatrix} -e^{i\beta}\cos\phi \\ -e^{i\beta}\sin\phi \\ 1 \end{pmatrix}, \tag{25}$$

where $\beta = \arg b$ and ϕ is the angle between vector $\mathbf{k}$ and the x axis.

When we denote the angle between $\mathbf{d}_m$ and the x axis by θ (see Fig. 3), we can easily show from the transformation properties by symmetry operations that

$$\left\langle \mathbf{u}_E^{(1)}(z_0)\cdot\mathbf{d}_m \right\rangle_0 = |\mathbf{d}_m|\langle u_{E,x}(z_0)\rangle_0 \cos\theta, \tag{26}$$

$$\left\langle \mathbf{u}_E^{(2)}(z_0)\cdot\mathbf{d}_m \right\rangle_0 = |\mathbf{d}_m|\langle u_{E,x}(z_0)\rangle_0 \sin\theta, \tag{27}$$

$$\left\langle \mathbf{u}_{A_1}(z_0)\cdot\mathbf{d}_m \right\rangle_0 = 0, \tag{28}$$

where

$$\begin{aligned}\langle u_{E,x}(z_0)\rangle_0 &= \frac{1}{V}\int_V d\mathbf{r}\, u_{E,x}^{(1)}(\mathbf{r})\delta(z-z_0) \\ &= \frac{1}{V}\int_V d\mathbf{r}\, u_{E,y}^{(2)}(\mathbf{r})\delta(z-z_0).\end{aligned} \tag{29}$$

Finally, for three solutions of $\Delta\lambda = 0$ and $\pm|b|k$, we obtain

$$\mathbf{S}_\parallel^{(0)} = \frac{\gamma_{\kappa 0}\omega_{\kappa 0}^2 |\mathbf{d}_m|^2 L_z |\langle \mathbf{u}_E(z_0)\rangle_0|^2 \mathbf{v}_{\kappa 0}}{4\mu_0\left\{(\omega-\omega_{\kappa 0})^2+\gamma_{\kappa 0}^2\right\}|\mathbf{v}_{\kappa 0}|}\sin^2(\phi-\theta), \tag{30}$$

$$\mathbf{S}_\parallel^{(\pm)} = \frac{\gamma_{\kappa\pm}\omega_{\kappa\pm}^2 |\mathbf{d}_m|^2 L_z |\langle \mathbf{u}_E(z_0)\rangle_0|^2 \mathbf{v}_{\kappa\pm}}{8\mu_0\left\{(\omega-\omega_{\kappa\pm})^2+\gamma_{\kappa\pm}^2\right\}|\mathbf{v}_{\kappa\pm}|}\cos^2(\phi-\theta). \tag{31}$$

In Eqs. (30) and (31),

$$|\mathbf{v}_{\kappa 0}| \approx 0 \quad \text{and} \quad \mathbf{v}_{\kappa\pm} = \pm\frac{v\kappa}{|\kappa|}, \tag{32}$$

where v is the slope of the Dirac cone.

Therefore, the quadratic mode with $\Delta\lambda = 0$ has a vanishing velocity in the vicinity of the Dirac point, which is a consequence of the quadratic $\mathbf{k}$ dependence of the eigenfrequency of the auxiliary dispersion surface, so its energy flow along the slab surface is small. On the other hand, Dirac-cone modes with $\Delta\lambda = \pm|b|k$ have a finite group velocity $\pm v$, so they propagate along the slab surface. Their propagation direction is parallel to the wave vector κ: The upper cone mode propagates in the κ direction and the lower cone mode propagates in the $-\kappa$ direction. An interesting feature is the presence of the $\cos^2(\phi-\theta)$ term in $\mathbf{S}_\parallel^{(\pm)}$, which was brought about by the anisotropic mixture of two dipolar wave functions, as shown in Eqs. (24) and (25). Due to this term, the induced energy flow along the slab surface is largest when the magnetic field of the incident plane wave is polarized in the same direction as κ.

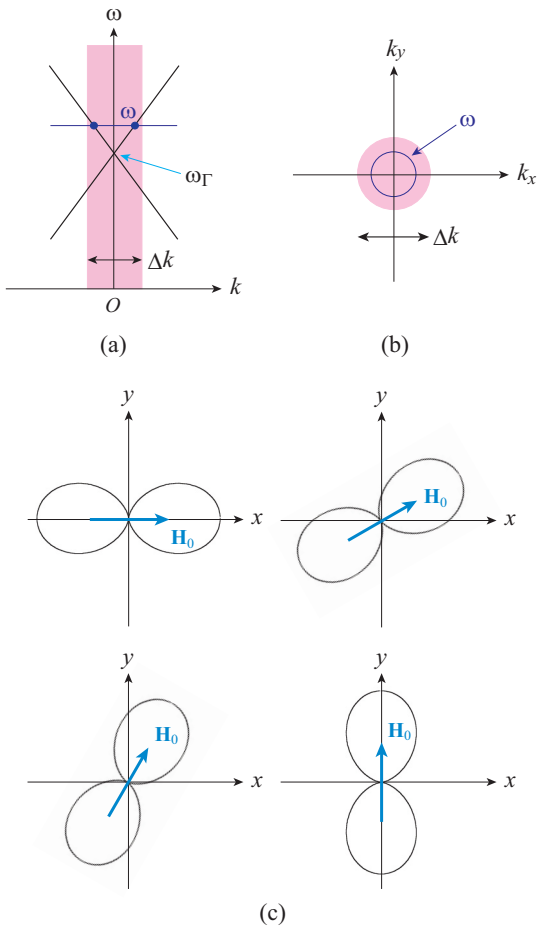

FIG. 4. (Color online) (a) The Dirac-cone modes (black dot) excited by an incident wave with frequency ω. Those modes have a wave vector in the range of $\Delta k = 2/w_0$. (b) The wave vector of the excited Dirac-cone mode resides on a circle in the $\mathbf{k}$ space, which is denoted by ω. Its radius is $|\omega-\omega_\Gamma|/v$. (c) Angular distribution of the energy flow of the excited Dirac-cone modes as a function of the (magnetic field) polarization angle of the incident wave.

Let us examine a realistic experimental situation here. In the experiments of the optical frequency range, we may use a laser as a monochromatic light source because of its good directivity. When we focus the laser beam on the slab specimen, it has a distribution of the lateral wave vector. When we approximate the focused beam by a Gaussian beam with a beam waist of diameter w_0, it has a distribution width of the lateral wave vector Δk:

$$\Delta k = 2/w_0. \tag{33}$$

So, we can excite all Dirac-cone modes whose wave vector is in this range. For simplicity, let us consider the normal incidence hereafter [Fig. 4(a)]. Then, the wave vector of the excited Dirac-cone modes resides on a circle in the $\mathbf{k}$ space [Fig. 4(b)]. When we use a linearly polarized light for excitation as we have described in this paper, those Dirac-cone modes whose wave vector is parallel to the direction of the polarization is excited most strongly according to Eq. (31). Therefore, we

TABLE I. The dependence of the energy flux $\mathbf{S}_{\parallel}$ on the polarization angle θ of the incident magnetic field and the propagation angle ϕ. The mode combinations listed in this table result in the formation of Dirac and double Dirac cones by accidental degeneracy for the C_{4v} and C_{6v} lattice structures [16]. "Silent" means that the coupling between the incident plane wave from the normal direction and the Dirac-cone mode is vanishing in the first-order approximation due to the symmetry of the relevant wave functions, so the Dirac-cone mode is not excited.

Lattice symmetry	Mode1	Mode2	Angular dependence
C_{4v}	E	A_1	$\cos^2(\phi-\theta)$
	E	A_2	$\sin^2(\phi-\theta)$
	E	B_1	$\cos^2(\phi+\theta)$
	E	B_2	$\sin^2(\phi+\theta)$
C_{6v}	E_1	E_2	1
	E_1	A_1	$\cos^2(\phi-\theta)$
	E_1	A_2	$\sin^2(\phi-\theta)$
	E_2	B_1	silent
	E_2	B_2	silent

can control the propagation direction of the Dirac-cone modes by changing the polarization of the incident wave as shown in Fig. 4(c) because the group velocity is parallel to the wave vector. This property can be used for identifying the Dirac-cone dispersion.

Other cases of the mode combinations that result in the formation of the Dirac cones by accidental degeneracy can be analyzed in a similar manner. In Ref. [16], we derived the matrix that defines the eigenequation in the first-order $\mathbf{k}\cdot\mathbf{p}$ perturbation for each mode combination that yields the Dirac cone. So, we can obtain the wave functions of the Dirac-cone mode as we did for the E and A_1 modes, and we can derive the angular dependence of the excited wave. The results are listed in Table I. As can be seen, each mode combination has its own angular dependence. Thus, we can distinguish the mode symmetry by measuring the angular distribution of the energy flux excited by the incident plane wave.

IV. TRIANGULAR LATTICE OF C_{6v} SYMMETRY

In this section, we examine the case of the triangular lattice of the C_{6v} symmetry, i.e., the symmetry of the regular hexagon

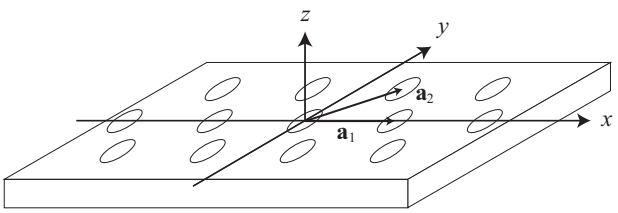

FIG. 5. Illustration of the triangular-lattice photonic-crystal slab of the C_{6v} symmetry, which is composed of a regular array of circular air cylinders fabricated in a uniform dielectric slab. Because the two-dimensional C_{6v} symmetry is sufficient for the Dirac cone, we do not assume a mirror symmetry about the horizontal middle plane.

(Fig. 5). The condition to materialize Dirac cones for this symmetry was analyzed by the tight-binding approximation [15] and by the vector $\mathbf{k}\cdot\mathbf{P}$ perturbation theory [16]. The most peculiar feature of this symmetry is the formation of the double Dirac cone without auxiliary quadratic dispersion surfaces, which is brought about by the degeneracy of eigenmodes of the E_1 and E_2 symmetries. Let us examine this case first.

The wave function and the eigenfrequency of the eigenmodes in the degenerate condition are given by solving the following eigenequation:

$$\begin{pmatrix} 0, & 0, & -bk_y, & -bk_x \\ 0, & 0, & -bk_x, & bk_y \\ -b^*k_y, & -b^*k_x, & 0, & 0 \\ -b^*k_x, & b^*k_y, & 0, & 0 \end{pmatrix} \begin{pmatrix} A \\ B \\ C \\ D \end{pmatrix} = \Delta\lambda \begin{pmatrix} A \\ B \\ C \\ D \end{pmatrix}, \tag{34}$$

where parameter b is given by

$$b = -i\mathbf{e}_y \cdot \big[-\langle \mathbf{u}_{E_1}^{(1)} | \Delta\mathcal{L} | \mathbf{u}_{E_2}^{(1)} \rangle_0 + \langle \mathbf{u}_{E_2}^{(1)} | \Delta\mathcal{L} | \mathbf{u}_{E_1}^{(1)} \rangle_0^* \big]. \tag{35}$$

The eigenwave function is given by

$$\mathbf{u}_{\mathbf{k}} = A\mathbf{u}_{E_1}^{(1)} + B\mathbf{u}_{E_1}^{(2)} + C\mathbf{u}_{E_2}^{(1)} + D\mathbf{u}_{E_2}^{(2)}. \tag{36}$$

Without the loss of generality, we can assume that the two eigenfunctions of the E_1 mode ($\mathbf{u}_{E_1}^{(1)}$ and $\mathbf{u}_{E_1}^{(2)}$) are transformed like the x and y coordinates by the symmetry operation of the C_{6v} point group, respectively, whereas those of the E_2 mode ($\mathbf{u}_{E_2}^{(1)}$ and $\mathbf{u}_{E_2}^{(2)}$) are transformed like $2xy$ and x^2-y^2, respectively [19]. The eigenvalues of Eq. (34) are

$$\Delta\lambda = \pm|b|k \quad \text{(double root)}. \tag{37}$$

The four solutions are

(i) $\Delta\lambda = |b|k$

$$\begin{pmatrix} A^{(+,1)} \\ B^{(+,1)} \\ C^{(+,1)} \\ D^{(+,1)} \end{pmatrix} = \begin{pmatrix} 1/\sqrt{2} \\ 0 \\ -e^{-i\beta}\sin\phi/\sqrt{2} \\ -e^{-i\beta}\cos\phi/\sqrt{2} \end{pmatrix}, \tag{38}$$

(ii) $\Delta\lambda = |b|k$

$$\begin{pmatrix} A^{(+,2)} \\ B^{(+,2)} \\ C^{(+,2)} \\ D^{(+,2)} \end{pmatrix} = \begin{pmatrix} 0 \\ 1/\sqrt{2} \\ -e^{-i\beta}\cos\phi/\sqrt{2} \\ e^{-i\beta}\sin\phi/\sqrt{2} \end{pmatrix}, \tag{39}$$

(iii) $\Delta\lambda = -|b|k$

$$\begin{pmatrix} A^{(-,1)} \\ B^{(-,1)} \\ C^{(-,1)} \\ D^{(-,1)} \end{pmatrix} = \begin{pmatrix} 1/\sqrt{2} \\ 0 \\ e^{-i\beta}\sin\phi/\sqrt{2} \\ e^{-i\beta}\cos\phi/\sqrt{2} \end{pmatrix}, \tag{40}$$

(iv) $\Delta\lambda = -|b|k$

$$\begin{pmatrix} A^{(-,2)} \\ B^{(-,2)} \\ C^{(-,2)} \\ D^{(-,2)} \end{pmatrix} = \begin{pmatrix} 0 \\ 1/\sqrt{2} \\ e^{-i\beta}\cos\phi/\sqrt{2} \\ -e^{-i\beta}\sin\phi/\sqrt{2} \end{pmatrix}. \tag{41}$$

From Eq. (17), we finally obtain the following based on a discussion similar to the previous section:

$$\mathbf{S}_{\parallel}^{(\pm,1)} = \frac{\gamma_{\kappa\pm}\omega_{\kappa\pm}^2|\mathbf{d}_m|^2 L_z \left|\langle \mathbf{u}_{E_1}(z_0)\rangle_0\right|^2 \mathbf{v}_{\kappa\pm}}{8\mu_0\left\{(\omega-\omega_{\kappa\pm})^2+\gamma_{\kappa\pm}^2\right\}|\mathbf{v}_{\kappa\pm}|}\cos^2\theta, \quad (42)$$

$$\mathbf{S}_{\parallel}^{(\pm,2)} = \frac{\gamma_{\kappa\pm}\omega_{\kappa\pm}^2|\mathbf{d}_m|^2 L_z \left|\langle \mathbf{u}_{E_1}(z_0)\rangle_0\right|^2 \mathbf{v}_{\kappa\pm}}{8\mu_0\left\{(\omega-\omega_{\kappa\pm})^2+\gamma_{\kappa\pm}^2\right\}|\mathbf{v}_{\kappa\pm}|}\sin^2\theta. \quad (43)$$

In the derivation of these two equations, we used

$$\langle \mathbf{u}_{E_2}(z_0)\cdot\mathbf{d}_m\rangle_0 = 0, \quad (44)$$

which can be proved by considering the spatial symmetry of the wave functions of the E_2 mode.

When we assume the same situation as shown in Fig. 4(a) that the specimen is irradiated by a Gaussian beam from the normal direction, all Dirac-cone modes at the incidence frequency whose wave vector resides on a circle in the reciprocal space are excited simultaneously. For the upper cone modes, for example, we have two modes for each κ, which are excited with an intensity proportional to $\cos^2\theta$ and $\sin^2\theta$, respectively. So their total intensity does not depend on the polarization angle θ or the propagation angle ϕ. Therefore, we should observe an isotropic propagation of excited waves along the slab surface, irrespective of the polarization of the incident wave for this case.

In addition to the double Dirac cone, a Dirac cone with an auxiliary quadratic dispersion surface can be formed by accidental degeneracy in the triangular lattice of the C_{6v} symmetry. The form of the eigenequation for each mode combination is given in Ref. [16]. So, we can obtain the wave functions of the Dirac-cone mode as before and can derive the angular dependence. The results are listed in Table I, where the Dirac cone formed by the accidental degeneracy of the E_2 mode is "silent" for the incident wave from the normal direction because the coupling between them is exactly equal to zero for the Γ point due to the symmetry mismatching and the coupling is also vanishing for small $\mathbf{k}$ in the first-order approximation. So, the Dirac-cone mode is not excited by the incident plane wave.

The eigenmode of photonic crystals is often observed as a dip in the angle-resolved reflection spectra. When this method is applied to the detection of Dirac cones, it may be difficult to accurately determine the dispersion relation in the vicinity of the Dirac point because there are two modes, i.e., upper and lower cone modes, whose frequencies are close to each other, so the two dips overlap. The propagation characteristics clarified in this paper can be used as another evidence for the Dirac cone and can be used to distinguish the mode symmetry. The isotropic and frequency-independent velocity is also evidence for the photonic Dirac cone.

V. CONCLUSION

We formulated a Green-function method to analyze the excitation process of Dirac-cone modes in photonic-crystal slabs by an incident plane wave. We obtained an analytic expression of Poynting's vector of the induced wave running parallel to the slab surface. By analyzing both the elements of the $\mathbf{k}\cdot\mathbf{p}$ perturbation matrix and the coupling strength between the incident wave and Dirac-cone modes by group theory, we clarified the dependence of the propagation intensity distribution on the polarization angle of the incident wave. We found that each mode combination shows its own angular dependence. We further analyzed the excitation process by a Gaussian beam in particular and showed that the propagation direction can be controlled by the polarization of the incident wave for the Dirac cone, whereas the intensity does not depend on the polarization for the double Dirac cone and its propagation intensity distribution is isotropic. These properties can be used for experimentally detecting Dirac cones and distinguishing their mode symmetry.

ACKNOWLEDGMENTS

This study was supported by MEXT KAKENHI Grant No. 22109007 and JSPS KAKENHI Grant No. 26610090.

APPENDIX A: RETARDED GREEN FUNCTION

In this section, we derive the retarded Green function for the magnetic field. We start with two of four Maxwell's equations:

$$\nabla\times\mathbf{E} = -\mu_0\frac{\partial\mathbf{H}}{\partial t}, \quad (A1)$$

$$\nabla\times\mathbf{H} = \varepsilon_0\varepsilon(\mathbf{r})\frac{\partial\mathbf{E}}{\partial t}, \quad (A2)$$

where $\mathbf{E}$ and $\mathbf{H}$ denote the electric and magnetic fields, respectively, μ_0 and ε_0 are the permeability and permittivity of free space, and $\varepsilon(\mathbf{r})$ is the periodic dielectric constant of the photonic-crystal slab,

$$\varepsilon(\mathbf{r}+\mathbf{a}_i) = \varepsilon(\mathbf{r}), \quad (A3)$$

where $\mathbf{a}_i$ $(i=1,\ 2)$ is an elementary lattice vector parallel to the surface of the photonic-crystal slab. The geometry for the square-lattice photonic-crystal slab, for example, is shown in Fig. 2. We assumed that the permeability of the photonic-crystal slab is the same as free space, since we do not deal with magnetic materials in this paper. By eliminating the electric field from Eqs. (A1) and (A2), we obtain

$$\mathcal{L}_H\mathbf{H} \equiv \nabla\times\left(\frac{1}{\varepsilon}\nabla\times\mathbf{H}\right) = -\frac{1}{c^2}\frac{\partial^2\mathbf{H}}{\partial t^2}, \quad (A4)$$

where operator $\mathcal{L}_H$ is defined by the first equality in Eq. (A4) and c is the speed of light in free space. To make our problem well defined, we assume that ε is real and independent of frequency and we impose the periodic boundary condition on $\mathbf{H}$. Then, we can prove by following similar discussions on the electric field in Ref. [17] and in Chap. 2 of Ref. [18] that $\mathcal{L}_H$ is Hermitian. The eigenfunctions of $\mathcal{L}_H$, which are composed of the transverse modes $\mathbf{H}^{(T)}$ and longitudinal modes $\mathbf{H}^{(L)}$, form a complete set. Their completeness is expressed by

$$\sum_{\mathbf{k},n}\mathbf{H}_{\mathbf{k}n}^{(T)}(\mathbf{r})\otimes\mathbf{H}_{\mathbf{k}n}^{(T)*}(\mathbf{r}') + \sum_{\mathbf{k},n}\mathbf{H}_{\mathbf{k}n}^{(L)}(\mathbf{r})\otimes\mathbf{H}_{\mathbf{k}n}^{(L)*}(\mathbf{r}') = VI\delta(\mathbf{r}-\mathbf{r}'), \quad (A5)$$

where I is the 3×3 unit matrix, V is the volume on which the periodic boundary condition is imposed, δ is Dirac's delta function, and $\mathbf{k}$ and n are the wave vector in the

two-dimensional first Brillouin zone and the band index, respectively. $\otimes$ denotes a tensor whose elements are given by the direct product of two vectors, i.e., $(\mathbf{A}\otimes\mathbf{B})_{ij}=A_iB_j$. $\mathbf{H}^{(T)}_{\mathbf{k}n}$ and $\mathbf{H}^{(L)}_{\mathbf{k}n}$ satisfy

$$\nabla\cdot\mathbf{H}^{(T)}_{\mathbf{k}n}=0, \tag{A6}$$

$$\nabla\times\mathbf{H}^{(L)}_{\mathbf{k}n}=0, \tag{A7}$$

respectively. We normalize them as

$$\left\langle\mathbf{H}^{(\alpha)}_{\mathbf{k}n}\middle|\mathbf{H}^{(\beta)}_{\mathbf{k}'n'}\right\rangle\equiv\int_V d\mathbf{r}\,\mathbf{H}^{(\alpha)*}_{\mathbf{k}n}(\mathbf{r})\cdot\mathbf{H}^{(\beta)}_{\mathbf{k}'n'}(\mathbf{r})=V\delta_{\mathbf{k}\mathbf{k}'}\delta_{nn'}\delta_{\alpha\beta}, \tag{A8}$$

where $\alpha,\beta=T$ or L and δ is Kronecker's delta. The inner product $\langle\cdots|\cdots\rangle$ is defined by the first equality of Eq. (A8). See Sec. 2.7 of Ref. [18] for the derivation of Eqs. (A5)–(A8). Note that we assumed the periodicity of the specimen structure only in the direction parallel to the slab surface, which we denote by the x and y coordinates, so the wave vector in the Brillouin zone is two dimensional and we generally denote it by

$$\mathbf{k}=(k_x,k_y,0). \tag{A9}$$

The retarded Green function in the frequency domain is given by

$$\mathcal{G}(\mathbf{r},\mathbf{r}',\omega)=\frac{c^2}{V}\sum_{\mathbf{k}n}\left[\frac{\mathbf{H}^{(T)}_{\mathbf{k}n}(\mathbf{r})\otimes\mathbf{H}^{(T)*}_{\mathbf{k}n}(\mathbf{r}')}{(\omega-\omega_{\mathbf{k}n}+i\delta)(\omega+\omega_{\mathbf{k}n}+i\delta)}+\frac{\mathbf{H}^{(L)}_{\mathbf{k}n}(\mathbf{r})\otimes\mathbf{H}^{(L)*}_{\mathbf{k}n}(\mathbf{r}')}{(\omega+i\delta)^2}\right], \tag{A10}$$

where δ is a positive infinitesimal to assure the causality and $\omega_{\mathbf{k}n}$ is the eigenangular frequency of $\mathbf{H}^{(T)}_{\mathbf{k}n}$. Note that the eigenfrequency of $\mathbf{H}^{(L)}_{\mathbf{k}n}$ is equal to zero from Eq. (A7). $\mathcal{G}(\mathbf{r},\mathbf{r}',\omega)$ satisfies

$$\left(\frac{\omega^2}{c^2}-\mathcal{L}_H\right)\mathcal{G}(\mathbf{r},\mathbf{r}',\omega)=I\delta(\mathbf{r}-\mathbf{r}'), \tag{A11}$$

which can be proved by using Eq. (A5). The retarded Green function in the time domain, which is defined by the inverse Fourier transform of $\mathcal{G}(\mathbf{r},\mathbf{r}',\omega)$, is given by

$$\begin{aligned}G(\mathbf{r},\mathbf{r}',t)&=\frac{1}{2\pi}\int_{-\infty}^{\infty}d\omega\,\mathcal{G}(\mathbf{r},\mathbf{r}',\omega)e^{-i\omega t}\\&=\begin{cases}-\frac{c^2}{V}\sum_{\mathbf{k},n}\left[\frac{\sin\omega_{\mathbf{k}n}t}{\omega_{\mathbf{k}n}}\mathbf{H}^{(T)}_{\mathbf{k}n}(\mathbf{r})\otimes\mathbf{H}^{(T)*}_{\mathbf{k}n}(\mathbf{r}')+t\mathbf{H}^{(L)}_{\mathbf{k}n}(\mathbf{r})\otimes\mathbf{H}^{(L)*}_{\mathbf{k}n}(\mathbf{r}')\right] & (t\geqslant 0),\\ 0 & (t<0).\end{cases}\end{aligned} \tag{A12}$$

It satisfies

$$-\left(\frac{1}{c^2}\frac{\partial^2}{\partial t^2}+\mathcal{L}_H\right)G(\mathbf{r},\mathbf{r}',t-t')=I\delta(\mathbf{r}-\mathbf{r}')\delta(t-t'), \tag{A13}$$

which can be confirmed by using Eq. (A11). The solution of the general inhomogeneous equation with a source term $\mathbf{F}$,

$$-\left(\frac{1}{c^2}\frac{\partial^2}{\partial t^2}+\mathcal{L}_H\right)\mathbf{H}(\mathbf{r},t)=\mathbf{F}(\mathbf{r},t), \tag{A14}$$

is given by the convolution

$$\mathbf{H}(\mathbf{r},t)=\int_V d\mathbf{r}'\int_{-\infty}^{\infty}dt'G(\mathbf{r},\mathbf{r}',t-t')\mathbf{F}(\mathbf{r}',t'), \tag{A15}$$

which can be proved by substituting Eq. (A15) into Eq. (A14) and using Eq. (A13).

APPENDIX B: RADIATION OF PLANE WAVES IN FREE SPACE

We derive the formula for the magnetic field emitted by the oscillating magnetic polarization in free space. By substituting Eq. (6) into Eq. (5), we obtain

$$\begin{aligned}\mathbf{H}(\mathbf{r},t)=&-\frac{\mathbf{P}_m(\mathbf{r},t)}{\mu_0}+\frac{e^{-i\omega t}}{4\pi\mu_0}\int_{-\infty}^{\infty}dk_z\,\mathbf{h}_\kappa(\mathbf{h}_\kappa\cdot\mathbf{d}_m)\omega_\kappa\\&\times e^{i(\kappa\cdot\mathbf{r}-k_zz_0)}\left(\frac{1}{\omega+\omega_\kappa+i\delta}-\frac{1}{\omega-\omega_\kappa+i\delta}\right),\end{aligned} \tag{B1}$$

where

$$\kappa=(\kappa_x,\kappa_y,k_z) \tag{B2}$$

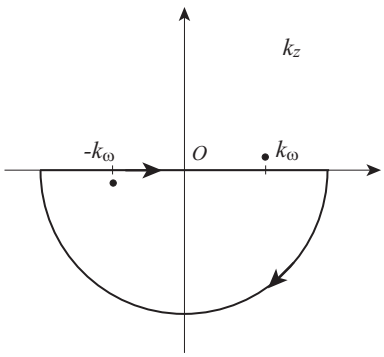

FIG. 6. The contour of the integral of Eq. (B1). The two poles are denoted by the black dots.

and $\mathbf{h}_\kappa$ is a unit vector perpendicular to κ and parallel to the plane spanned by $\mathbf{d}_m$ and κ. Since there is a factor $e^{ik_z(z-z_0)}$ and we consider the region $z < z_0$, we can close the path of the integral in Eq. (B1) in the lower half of the complex k_z plane, as shown in Fig. 6. The first term in the parentheses on the right-hand side of Eq. (B1) does not yield a pole for the k_z integral, whereas the second term yields two poles at

$$k_z = \pm k_\omega \equiv \pm\sqrt{\frac{\omega^2}{c^2} - \kappa_x^2 - \kappa_y^2}. \tag{B3}$$

The pole at $-k_\omega$ is included in the contour and its residue is $\omega/c^2 k_\omega$. Then, from the residue theorem, we obtain

$$\mathbf{H}(\mathbf{r},t) = -\frac{\mathbf{P}_m(\mathbf{r},t)}{\mu_0} + \frac{i\,\mathbf{e}_{\mathbf{k}_0}\left(\mathbf{e}_{\mathbf{k}_0}\cdot\mathbf{d}_m\right)\omega\sqrt{\omega^2 - c^2\kappa_x^2}}{2\mu_0 c^2 k_\omega} \times e^{i(\mathbf{k}_0\cdot\mathbf{r}-\omega t)+ik_\omega z_0}. \tag{B4}$$

For $\kappa_x = \kappa_y = 0$ in particular,

$$\mathbf{H}(\mathbf{r},t) = -\frac{\mathbf{P}_m(\mathbf{r},t)}{\mu_0} + \frac{i\omega\,\mathbf{d}_m}{2\mu_0 c}\, e^{-i(\omega/c)(z-z_0+ct)}. \tag{B5}$$

[1] F. D. M. Haldane and S. Raghu, Phys. Rev. Lett. **100**, 013904 (2008).
[2] S. Raghu and F. D. M. Haldane, Phys. Rev. A **78**, 033834 (2008).
[3] T. Ochiai and M. Onoda, Phys. Rev. B **80**, 155103 (2009).
[4] X. Zhang, Phys. Rev. Lett. **100**, 113903 (2008).
[5] L.-G. Wang, Z.-G. Wang, and S.-Y. Zhu, Europhys. Lett. **86**, 47008 (2009).
[6] R. A. Sepkhanov, Y. B. Bazaliy, and C. W. J. Beenakker, Phys. Rev. A **75**, 063813 (2007).
[7] M. Diem, T. Koschny, and C. M. Soukoulis, Physica B **405**, 2990 (2010).
[8] Zheng Wang, Yidong Chong, J. D. Joannopoulos, and Marin Soljačić, Nature (London) **461**, 772 (2009).
[9] M. Hafezi, S. Mittal, J. Fan, A. Migdall, and J. M. Taylor, Nat. Photon. **7**, 1001 (2013).
[10] X. Huang, Y. Lai, Z. H. Hang, H. Zheng, and C. T. Chan, Nat. Mater. **10**, 582 (2011).
[11] J. Mei, Y. Wu, C. T. Chan, and Z.-Q. Zhang, Phys. Rev. B **86**, 035141 (2012).
[12] M. Silveirinha and N. Engheta, Phys. Rev. Lett. **97**, 157403 (2006).
[13] A. Alu, M. G. Silveirinha, A. Salandrino, and N. Engheta, Phys. Rev. B **75**, 155410 (2007).
[14] K. Sakoda, Opt. Express **20**, 3898 (2012).
[15] K. Sakoda, Opt. Express **20**, 9925 (2012).
[16] K. Sakoda, Opt. Express **20**, 25181 (2012).
[17] K. Sakoda and K. Ohtaka, Phys. Rev. B **54**, 5732 (1996).
[18] K. Sakoda, *Optical Properties of Photonic Crystals*, 2nd ed. (Springer-Verlag, Berlin, 2004).
[19] T. Inui, Y. Tanabe, and Y. Onodera, *Group Theory and Its Applications in Physics* (Springer, Berlin, 1990).